Physics of a Thick Seasonal Snowpack with Possible Implications for Snow Algae

Authors: Dove, Adrienne, Heldmann, Jennifer, McKay, Christopher, and Toon, Owen B.

Source: Arctic, Antarctic, and Alpine Research, 44(1) : 36-49

Published By: Institute of Arctic and Alpine Research (INSTAAR), University of Colorado

URL: https://doi.org/10.1657/1938-4246-44.1.36

Arctic, Antarctic, and Alpine Research, Vol. 44, No. 1, 2012, pp. 36–49

Physics of a Thick Seasonal Snowpack with Possible Implications for Snow Algae

Adrienne Dove‡*
Jennifer Heldmann†
Christopher McKay† *and*
*Owen B. Toon**

*Laboratory for Atmospheric and Space Physics, 1234 Innovation Drive, Boulder, Colorado 80303-7814, U.S.A.
†NASA Ames Research Center, Division of Space Sciences and Astrobiology, NASA Ames Mail Stop 245-3, Mountain View, California 94035, U.S.A.
‡Corresponding author: adrienne.dove@colorado.edu

Abstract

Instrumentation to study snowpack *in situ* was deployed in Lassen Volcanic National Park (LVNP), California, in an area of deep seasonal snow accumulation and known snow algal bloom recurrence. Included in the instrumentation were 11 temperature sensors, evenly spaced up to 2 m above the ground, which provided (1) temperature data within the snowpack when buried, and (2) estimates of snowpack height during accumulation and ablation periods. Beginning in April, moisture sensors measured a strong increase of snowpack liquid water content to greater than 15% by volume; this high melt content is usually coincident with the start of runoff from the snowpack. Snow depth profiles showed a rapid ablation of the final 2 m of the snowpack over about 23 days beginning in late June. SNTHERM numerical modeling confirmed that solar radiation was the dominant energy term throughout the melt season. By modeling a variety of snowpack parameters, such as albedo and initial snow density, we determined that the date of snow loss is the most sensitive observable that can be used to constrain the modeled parameters. These data sets from LVNP can also be applied to knowledge of snow algae lifecycles in deep snow to help understand whether the availability of light, water, or both controls the onset of snow algae germination at the base of a thick snowpack. Data and modeling indicate that meltwater was present throughout the snowpack beginning in March and runoff is initiated in April, when the snowpack was still several meters deep. However, significant levels of light did not penetrate to the soil until June, when the snow was less than 2 m deep.

http://dx.doi.org/10.1657/1938-4246-44.1.36

Introduction

Thick, seasonal snowpacks occupy an interesting zone within types of snow cover, falling in the realm between thin, transient snow covers and permanent snowfields and glaciers. These deep snowpacks offer a chance to study the physics that govern snow metamorphism and melt processes, since many different environments exist within thick snowpacks. The top layers interact with the atmosphere and experience the same energy exchanges as shallower snowpacks, while the layers at depth are insulated from these effects, only exchanging energy with surrounding snow layers or melt water and, for the very lowest layers, with the underlying soil surface.

In our changing global environment, there is a need to understand water resources, and how both human-induced and natural effects modify these resources. Snow dominates the hydrological processes operating in many regions, with snowmelt determining the availability and timing of runoff downstream. Barnett et al. (2008) found that 60% of the climate-related trends in snow cover, winter air temperature, and river flow changes over the last 50 years have been human-induced, meaning that these hydroclimatic changes differ in length and strength from expected natural variability in ways consistent with human-induced effects. Snow cover duration is the variable most sensitive to changes in climate, especially in the coastal mountains of North America (Déry and Brown, 2007; Brown and Mote, 2008). The presence of snow cover dramatically affects the planetary albedo, with a strong positive feedback mechanism between snow, albedo, and radiation balance. The most significant effect of changes in snow duration on the radiation balance occurs in the spring (Groisman et al., 1994; Déry and Brown, 2007). Increased daily minimum temperature due to greenhouse warming is shown to be statistically associated with a smaller percentage of precipitation falling as snow, earlier runoff, and shortened snow cover duration (Barnett et al., 2008; Déry and Brown, 2007).

Several approaches have been taken to studying snow-covered surfaces. One technique is to gather field data, often in campaigns throughout a snow season, at one or many specific sites. While creating a study in spatial variability of snow cover, these data sets are snapshots in time, with little temporal coverage. Meteorological data can be combined with this approach, and the two are often used in conjunction with numerical modeling to better understand the physical processes occurring in the snowpack (i.e. Cline, 1997a, 1997b; Elder et al., 2009a, 2009b; Hayashi et al., 2005). Spacecraft or airborne sensors can provide another spatially distributed data set and can measure a wide variety of parameters that describe the snow cover (Cline et al., 2009; Painter et al., 2001), but none of these data provide continuous temporal coverage. Recently, Tyler et al. (2008) used distributed temperature sensing (DTS) to measure spatial variability of basal snowpack temperatures with resolutions of 1 m, 10 s, and 0.1 °C. These systems are expensive, however, and have been limited to horizontal transects along the ground, though vertical profiling was suggested in Selker et al. (2006). Lundquist and Lott (2008) also studied temperature variability at the snow-soil interface, finding that small, inexpensive, self-recording temperature sensors can be useful for long-term monitoring of spatial snow distributions.

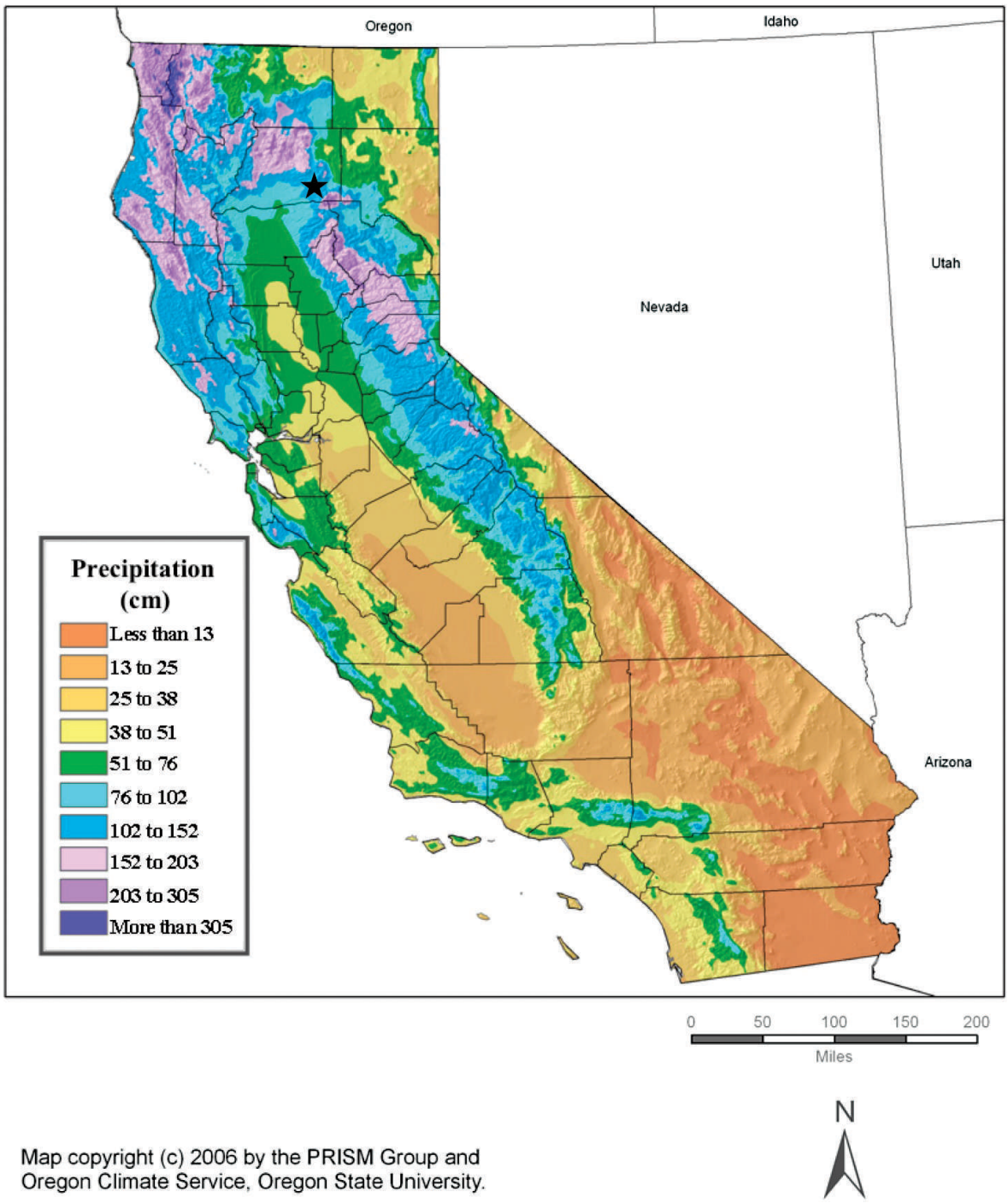

FIGURE 1. Annual average precipitation. Map constructed by the PRISM Climate Group (formerly the Spatial Climate Analysis Service) at Oregon State University. The star indicates the location of Lassen Volcanic National Park (LVNP), and the legend was modified to indicate precipitation in centimeters rather than inches.

Changes in biomass and in the locations of microbial populations may also be sensitive indicators of climate change effects on a region (Yoshimura et al., 1997; Painter et al., 2001). Snow algae are green algal flagellates (*Chloromonas* and *Chlamydomonas*) that have been identified and investigated in a variety of locations around the world (e.g., Hardy and Curl, 1972; Hoham, 1980; Müller et al., 2001; Painter et al., 2001) to explore their physical characteristics and the environmental factors that trigger their germination. Studies have shown that snow algal spores lie dormant on the ground throughout most of the year, until either meltwater in the snowpack trickles down to the surface, until light levels are high enough to trigger germination and initiate migration up through the snowpack toward the sunlight, or both (Hoham and Ling, 2000). Curl et al. (1972) found that light levels

TABLE 1

Lassen Peak, Lake Helen (2515 m), 1930–2004 monthly snowfall data (centimeters). Compiled from data available from the California Cooperative Snow Surveys.

	Jan	Feb	March	April	May
Average	208	310	381	452	409
Minimum	48	61	94	163	97
Maximum	399	564	691	841	772

of 0.1% of full surface sunlight corresponded to the first spring bloom and suggested that increasing light penetration may initiate germination of the overwintering stages. In a series of papers, Hoham and colleagues (see Hoham and Ling, 2000, and references therein) reported that snow temperatures at the melting point and snow water contents between 40 and 70% (mL H_2O from 100 cm^3 of snow) were characteristic of colonized snow in thin snowpacks. Because of their sensitivity to the light and moisture content of a snowpack, snow algae will be especially susceptible to changing snowpack conditions due to climate change. This may affect the onset of germination as well as the length of time in which conditions are suitable for the organisms to complete a lifecycle.

We have developed a low-cost, low-maintenance, freestanding instrumentation structure with which to measure snowpack parameters at various depths within a snowpack continuously throughout an entire snow cover season. Using this instrumentation, we have observed thick snowpacks at a field site in Lassen Volcanic National Park, California, over several field seasons. Data recorded at the field site provides profiles of temperature, moisture, and light within the snow, as well as amount and timing of runoff. Snowpacks in this area have been observed to be sites of annual snow algae activity with rich red layers in the snow virtually every summer (Steve Zachary, personal communication). Snow algae are present throughout the mountains in western North America, including other sites around Lassen Volcanic National Park (Wharton and Vinyard, 1983). After the snow melts the resting stages of the snow algae are visible on the surface rocks and soils. Snow algae are of astrobiological interest because of an ability to thrive in extreme cold and high ultraviolet radiation conditions; for this reason, they have been proposed as a model for life in snowfields on Mars (Edwards et al., 2004). Long-term studies at this site may contribute to understanding the response of thick snow covers and their associated microorganisms to the impact of climate warming over the next few decades (Déry and Brown, 2007).

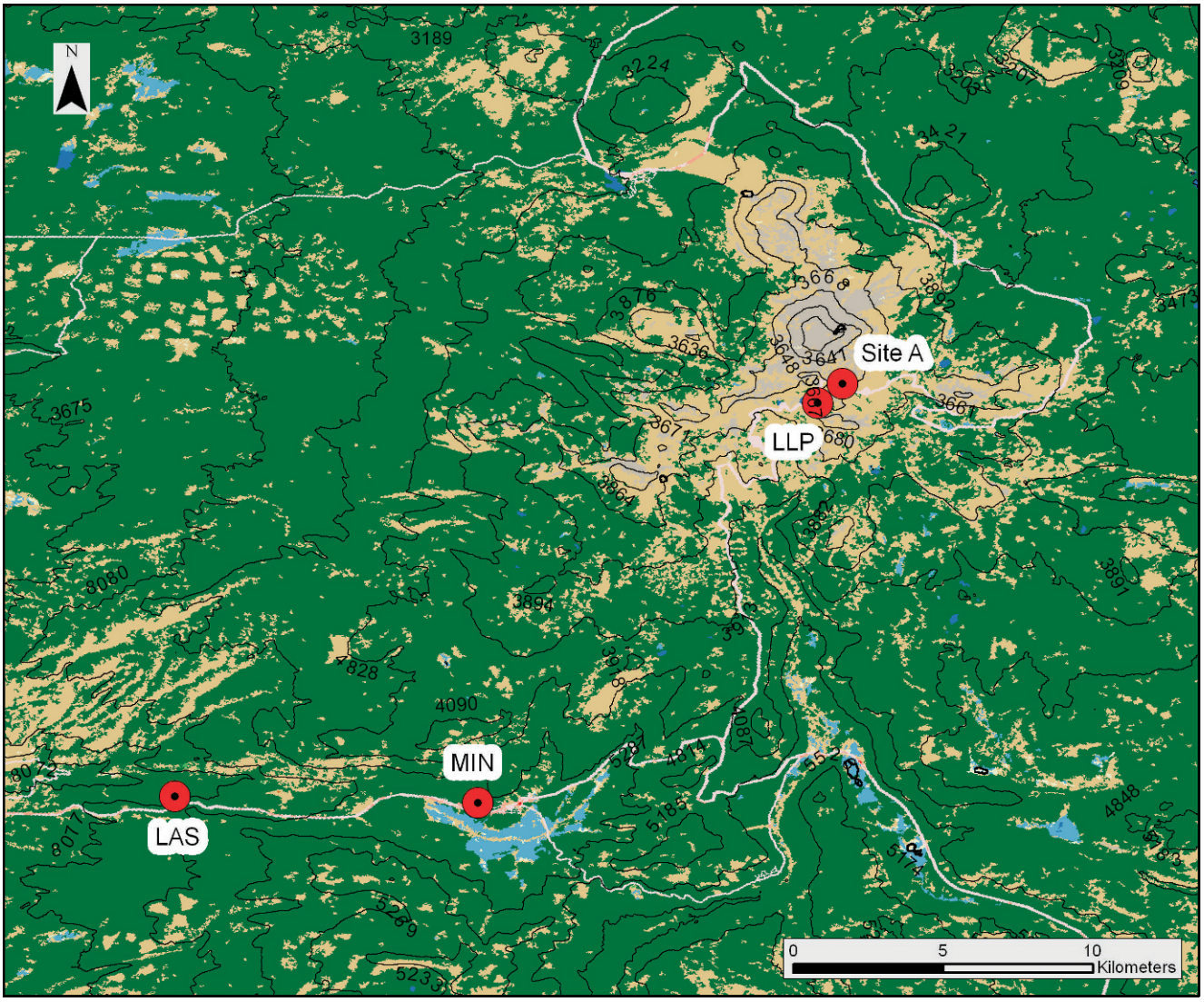

FIGURE 2. Topographic map of the regions surrounding the fieldsite, with the fieldsite and locations of the three meteorological sites marked (see also Table 3).

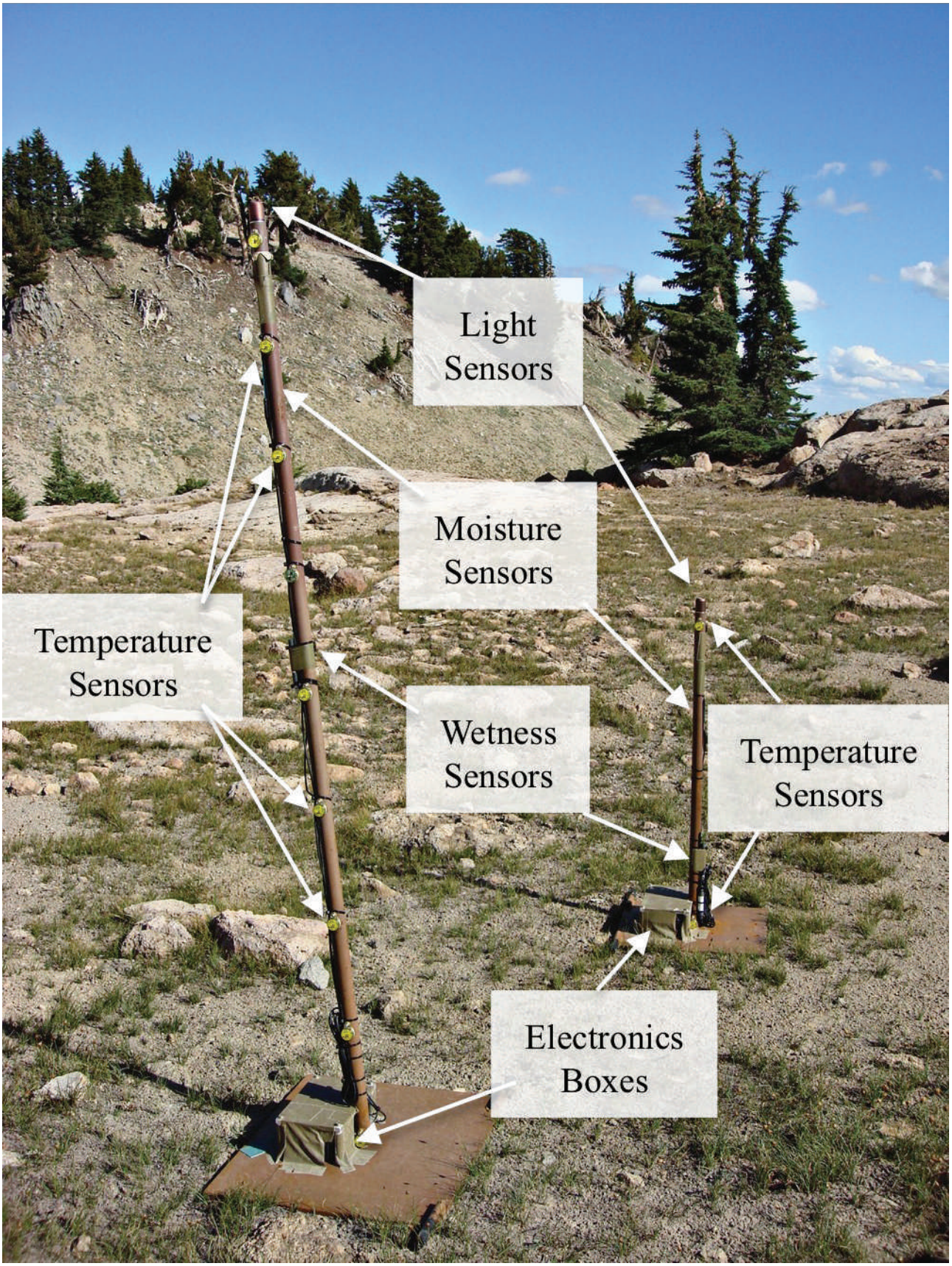

FIGURE 3. Instrumentation at Lassen field site. Not pictured are the collection bucket and tipping rain gauge, or the camera overlooking the site. The post in the foreground is approximately 2 m tall and the shorter post in the background is approximately 1 m tall.

TABLE 2

Instrument Specifications.

	Range	Accuracy	Resolution
StowAway TidbiT Model TBI32-20+50	−20 to +50 °C	≤0.55 °C (temperature dependent)	difference between temperature steps (varies)
Photosynthetically Active Radiation (PAR) Smart Sensor	0 to 2500 μmol/m^2/sec, wavelengths 400 to 700 nm	±5 μmol/m^2/sec	2.5 μmol/m^2/sec
Leaf Wetness Smart Sensor	0% (dry) to 100% (wet)	repeatability ±5%	0.59%
Soil Moisture Smart Sensor	0.0 to 0.450 m^3/m^3 (0 to saturated volumetric water content)	±0.041 m^3/m^3	±0.0006 m^3/m^3 (±0.06%)
HOBO Weather Station Rain Gauge Smart Sensor(w/tipping bucket mechanism)	10 cm/hr	±1.0% at up to 20 mm/hr	0.2 mm
HOBO Micro Station Data Logger	Operational temperatures: −20 to +50 °C	Time accuracy: ±5 s/week at 25 °C	N/A
HOBO Pro Series Datalogger, Temp/RH	RH: 0–100% Temperature: −30 to +50 °C	RH: ±3% Temperature: ±0.2 °C (high-resolution) ±0.4 °C (standard)	RH: (1%)* Temperature: 0.02 °C (high-resolution) 0.38 °C(standard)
Campbell CC640 Digital Camera with CompactFlash memory card	512 Mb memory		640 × 480 640 × 504 (with Time Stamp banner)

* Not in specifications, but output is in integer intervals.

This paper describes the observations and modeling used in this effort to utilize a new approach to *in situ* snowpack measurement. First, we describe the fieldsite and instrumentation, and then present the results from both the observations and corresponding modeling efforts. Finally, we discuss these results and insight gained into the instrumentation, thick snowpacks and their relevant physics, and possible implications for the relationship between snow algae development and snowpack metamorphosis.

Methods

SITE DESCRIPTION

Lassen Volcanic National Park (LVNP) is located in northern California at the southern end of the Cascade Range. The area is an active geothermal region; Lassen Peak last erupted in 1917, and there are many geothermal venting regions within LVNP (Lassen Volcanic National Park, National Park Service, http://www.nps.gov/lavo/index). Precipitation in this region primarily occurs as snowfall, with snow cover generally present beginning in late September and lasting until late July or August. Some higher elevations regions, such as Lassen Peak, can have snow year-round. Data taken at a Lake Helen meteorological site (40.468°N, 121.507°W) since the 1930s indicates that Lassen routinely records some of the greatest snow depths in California, as it is not in the precipitation shadow of any of the surrounding mountains. Figure 1 depicts averaged annual precipitation (predominantly snowfall) in northern California, and snowfall averages, minima, and maxima for the Lake Helen site are shown in Table 1.

TABLE 3

Instrumentation and meteorological data site locations. Lassen Site A is our fieldsite, while the other three are nearby meteorological stations maintained by the California Department of Water Resources.

Site	Latitude (°N)	Longitude (°W)	Elevation (m)	Met variables used
Lassen Site A	40.474	121.500	2560	Temperature
Lower Lassen Peak	40.468	121.507	2515	Wind Speed
Lassen Lodge	40.350	121.700	1256	Relative Humidity
Mineral	40.348	121.609	1510	Precipitation

Instrumentation was placed at a fieldsite (Site A) located at 40.474°N, 121.500°W, at about 2550 m above sea level. The fieldsite and the three meteorological data site locations are presented in Figure 2 and Table 3. The site was approximately 1 km to the east and just over a small ridge from Lake Helen, approximately at the tree line, with only low-lying brush present in the equipment area. As observed at Lake Helen, the fieldsite experiences heavy snowfall events, with snow depths greater than 10 m in some years (Steve Zachary, personal communication). As discussed above, this site had a thick but strictly seasonal snowpack and annual recurrences of snow algae. Instrumentation was first deployed at the field site in 2006 and was subsequently revised and redeployed yearly in the fall. The site was inaccessible throughout most of the winter and spring because of the depth of the snow and avalanche danger.

INSTRUMENTATION

Instruments were deployed on a tall and a short post that were 2 m and 1 m in height, respectively (refer to Fig. 3 for relative proportions and instrument locations). The short post was located 1.6 m from the tall post, in a roughly southerly direction. StowAway TidbiT temperature loggers were fixed with epoxy along the length of both posts; nine TidbiTs were placed on the tall post at 0.01 m, 0.27 m, 0.52 m, 0.77 m, 1.02 m, 1.27 m, 1.52 m, 1.74 m, and 1.96 m above the metal base of the post (Fig. 3), and two TidbiT sensors were placed on the short post at 0.01 m and 0.96 m above its metal base. Photosynthetically Active Radiation (PAR) Smart Sensors were placed at the top of each post, at 2.04 m and 1.04 m. A Leaf Wetness Smart Sensor (which detects the percentage wetness coverage of a sensor surface) was placed on each post, 1.17 m and 0.30 m above the base of the tall and short posts, respectively. Similarly, an ECHO Soil Moisture Smart Sensor (which detects changes in the dielectric constant of the surrounding material due to water) was placed 1.69 m and 0.68 m above the base of the tall and short posts, respectively. Instrument specifications and accuracies are given in Table 2. All data were recorded hourly. The wetness sensor and the moisture sensor provide complimentary data on the presence of liquid water. The wetness sensor is especially sensitive to the presence of liquid water due to marked changes in electrical conductivity when the liquid phase is present; however, it is primarily a qualitative indicator

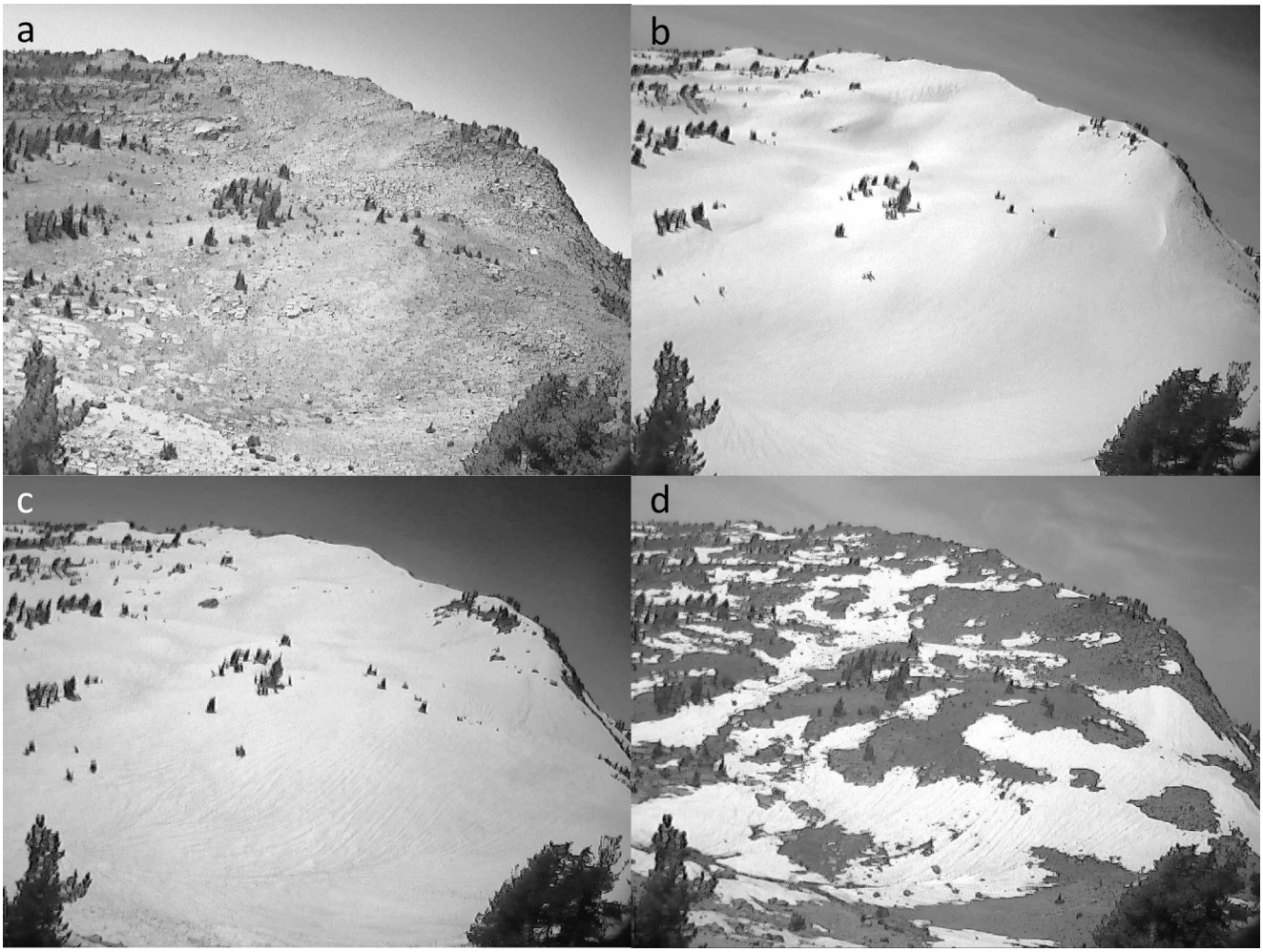

FIGURE 4. Images of the fieldsite throughout the 2007–2008 season, taken from the camera overlooking the fieldsite. (a) Fieldsite without snow, 9 August 2008. (b) Near time of maximum snow depth, 11 March 2008. (c) After melt has begun, 16 May 2008. (d) A few days before final snowmelt, 30 June 2008.

and not readily quantified (see McKay et al., 2003). The ECHO moisture sensor is less sensitive at low water levels than the wetness sensor but provides a quantifiable measurement of the liquid water content in the volume surrounding the sensor. Data from the PAR, Leaf Wetness, and Soil Moisture sensors were recorded by a HOBO Micro Station Datalogger, housed in a waterproof box at the base of each post. Each line into the box was sealed with epoxy to prevent the intrusion of water into the datalogger and electronics.

Additional data were collected by a HOBO Weather Station Rain Gauge Smart Sensor, located several meters south of the two posts under a snow collection tray. When covered by snow, this sensor also provides information on runoff that percolates through the base of the snowpack. For contextual information about the field site, a Campbell CC640 Digital Camera was placed on a hillside overlooking the equipment set-up and programmed to take an image daily at noon local time. Figure 4 shows images taken at four times during the season, illustrating the varied coverage and snow conditions. The ventilated camera box was positioned near brush so that both the box and its contents were somewhat shielded from direct solar radiation. A HOBO Pro Series Temperature/RH sensor was placed inside of the box to record temperature measurements.

This paper will focus on the data obtained during the 2007–2008 field season. Instruments were deployed in late October 2007 when there was patchy snow cover in certain locations in the park, but no snow at the site of the equipment. The temperature, moisture, and radiation sensors all began recording data on 1 November 2007, while camera images were taken beginning on 22 October 2007. All TidbiT loggers recorded data until they were collected from the site on 17 August 2008. The MicroStation on the tall post continued to record hourly values from the PAR and Soil Moisture sensors until the data were downloaded on 17 August 2008, but the Leaf Wetness sensor broke off of its base during the snow season (part of the sensor was found lying on the base of the post). The MicroStation on the short post recorded hourly data until 15 May 2008; the station ceased recording when the batteries ran out of power. Camera observations continued until the data were downloaded from the CompactFlash drive on 18 August 2008.

NUMERICAL MODELING

Numerous models have been developed to describe mass- and energy-balance within terrestrial snowpacks. These models range in complexity from one-layer energy transport to multi-layer distributed models. SNTHERM is an example of a physically based, one-dimensional mass- and energy-balance model used for computing temperatures and energy flux profiles within a snowpack (Jordan, 1991). It is a widely-used, publicly distributed code that has been repeatedly tested and shown to reproduce

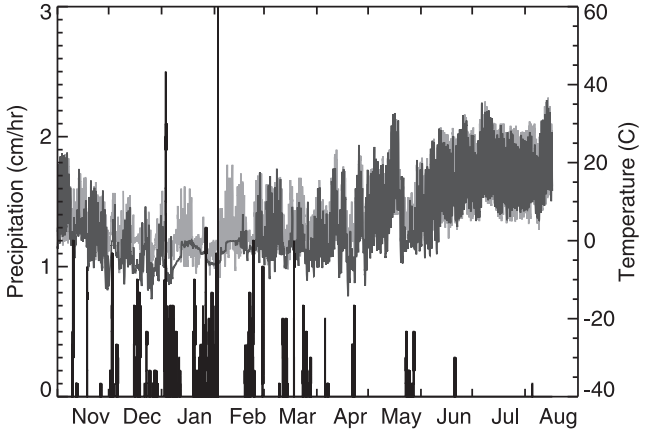

FIGURE 5. Hourly temperature (dark gray lines, right axis) and precipitation data (black bars, left axis) from a representative meteorological input file. In this case, temperature is taken from the camera box and is not scaled, and the precipitation is 1.9 times that reported at the Mineral weather station. The hourly temperature data from the Mineral weather station is also shown in light gray (right axis).

accurate temperatures, energy fluxes, and melt timing. For instance, Jin et al. (1999) have shown that SNTHERM performs well against other models in reproducing observations of snow in the Sierra Nevada mountains, and the model has been used to compute energy balances in mid-latitude, continental alpine snowpacks with good fidelity (Cline, 1997a, 1997b).

SNTHERM simulations were run for an entire snow season at our field site in LVNP, from bare soil just before initial snow deposition, through the transition to snow-covered ground, freeze-thaw cycles, the end-of-season ablation and melt, and return to bare soil. Simulations were initialized with a representative profile of soil temperature, bulk water content, and grain size for snow and soil layers and with the meteorological boundary conditions throughout the period to be modeled. Air temperature data were taken from the camera box overlooking the fieldsite, which remained exposed throughout most of the season. Relative humidity, wind speed, and precipitation data were obtained from measurements taken at nearby meteorological sites controlled by the California Department of Water Resources (accessed 23 December 2010) (available to download from the Department of Water Resources California Data Exchange Center [CDEC], http://cdec.water.ca.gov). The location and elevation of each site are listed in Table 3 and shown in Figure 2. Representative temperature and precipitation input data are shown in Figure 5.

Solar radiation data were taken from the PAR light sensors at the site, which measure incident radiation in the 400–700 nm region of the spectrum. This radiation is essential for biological activity, so that it is useful to measure this range for coincident snow algal population studies. However, snow energy-balance models are driven using the total incoming solar radiation, which is comprised of a much larger portion of the spectrum (typical pyranometers detect solar radiation in the range 310–2800 nm). We first converted the PAR radiation, measured in $\mu mol/m^2/s$ to W/m^2 using a conversion factor of 4.6 (Baker, 2001). This value was then converted to total incident solar radiation, assuming that PAR radiation made up about 49% of the total (Stanhill and Fuchs, 1977). Because the sensors were buried for part of the season, the data were supplemented with estimates using a simple cosine function that is modified for cloudy days.

Results

OBSERVATIONAL DATA

Data collection at the Lassen fieldsite allowed us to observe events that add to our knowledge of the interior conditions of the snowpack. Light, temperature, moisture, and wetness sensors provided meteorological data when they were exposed to the ambient atmospheric conditions, and their responses indicated which days were clear and which experienced precipitation events. When the sensors were buried we obtained profiles of the conditions in the snowpack interior, including how these measured parameters changed throughout the snow metamorphosis. Camera observations supplemented the sensor data and were especially useful for glimpsing a snapshot of the daily weather conditions, in addition to providing context of snow depth, distribution, and surface conditions around the fieldsite (Fig. 4). The tipping bucket runoff sensor provided further constraints on the timing and amount of runoff from the snowpack at the end of the season.

Temperature sensors provided the most useful information about the interior of the snowpack, and we used temperature profiles to estimate the snow depth throughout the season. Distinct diurnal variations were observed when a temperature sensor was exposed to the ambient atmospheric conditions, but these variations were damped when the sensor was covered in snow. Observations such as these have been used in other studies to determine both horizontal spatial coverage and snow depth (Taras et al., 2002; Lundquist and Lott, 2008). Assuming average values for the thermal properties of snow taken from Arya (2001), the diurnal thermal skin depth in the snow was estimated to be approximately 0.1 m or less. Additional constraints were placed on the overlying snowpack depth based on the other TidbiT sensors, as well; these sensors were spaced 0.25 m apart, making it possible to compare the magnitude of the observed temperature variations.

We calculated the change in the snowpack depth with time by observing the date that each temperature sensor was buried. After the uppermost sensor was buried, we lost the ability to discern further changes in the snowpack height. Instead, while the sensors were buried we observed the change in temperature of the snowpack as it equilibrated and eventually became isothermal at 0 °C at all measured depths, as seen in Figure 6. At this point, there was likely liquid water (melt) present throughout the snowpack. The snowpack then remained at 0 °C until it melted away. Depth change information was again available during the melt season. Then, the rate of snowpack depletion (change in height with time) was determined by observing when the temperature sensors measured strong diurnal variations. The period of sensor burial and the length of time each sensor on the tall post remained buried is shown in Table 4.

ECHO moisture and wetness (electrical conductivity) sensors provided complementary data about the liquid water content of the snowpack at four heights (Fig. 7, parts a and b). The wetness sensors were buried earlier in the season than the moisture sensors because they were placed lower on each post. All four of these sensors showed sharp increases on days corresponding to precipitation events early in the season (i.e. 2 December 2007). The lower wetness and moisture sensor measurements began to diverge significantly from the readings of the higher sensors after the snowfall event on 6 December 2007, although the lower wetness sensor was probably not buried deeply until the snowfall event on 16 December 2007 when the measurements indicated the start of a gradual and continuous rise in moisture content. There was a sharp increase in the lower sensor moisture content on 17 December 2007, after which there was a gradual rise in the

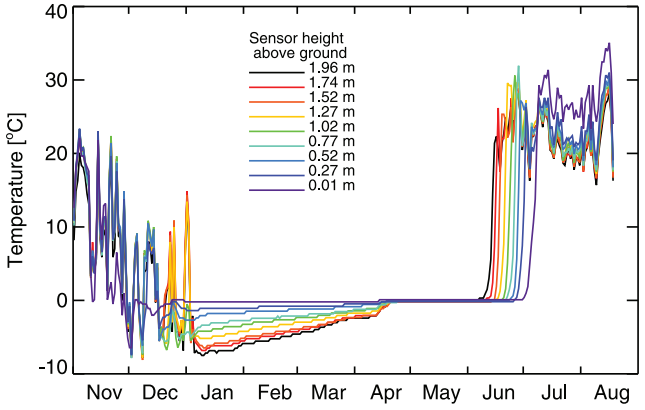

FIGURE 6. Hourly temperature data from the TidbiT temperature sensors on the tall post for the entire field season.

measurements. Both of the upper sensors were buried around 3 January 2008 (when there was a spike in the moisture data), after which both sensors recorded a gradual rise.

We interpret the rising values of both moisture sensors during the time after burial as an indication of increasing water content throughout the snowpack, and both wetness sensors eventually reached and retained saturated readings, indicating the presence of liquid water. The prediction of runoff could not be supported by rain gauge data during that time because the rain gauge did not record tips due to liquid runoff for the majority of the season. We believe the bucket's movement was impeded due to the presence of snow, or some other factor. In previous seasons, however, we observed that rain gauge data indicative of runoff showed a correlation with the timing of increases in the moisture and wetness sensor data, which supports our interpretations from this season of high liquid water content and runoff. The sharp increase in moisture content that began on 14 April 2008 may have corresponded with the onset of runoff through the snowpack. The upper wetness sensor measurements dropped to zero percent on 9 May 2008, which corresponded to maxima observed by the moisture sensors and may have been an indication of sensor saturation or of runoff from the snowpack. An additional spike in wetness on 20–21 June 2008 was likely due to changes within the wet snow, as the sensors remained covered. An increase in the moisture content measured by the upper moisture sensor was present on this day as well.

NUMERICAL MODELING

SNTHERM models were run in order to reproduce the observed snowpack growth and ablation rates and melt timing.

TABLE 4

Dates of snow cover and removal for the observed field season.

Height (m)	Period Buried	Total Days Buried
1.96	5 January–14 June	163
1.74	5 January–17 June	165
1.52	5 January–18 June	166
1.27	4 January–21 June	170
1.02	19 December–24 June	188
0.77	18 December–27 June	192
0.52	17 December–28 June	194
0.27	15 December–1 July	199
0.02	2 December–6 July	217

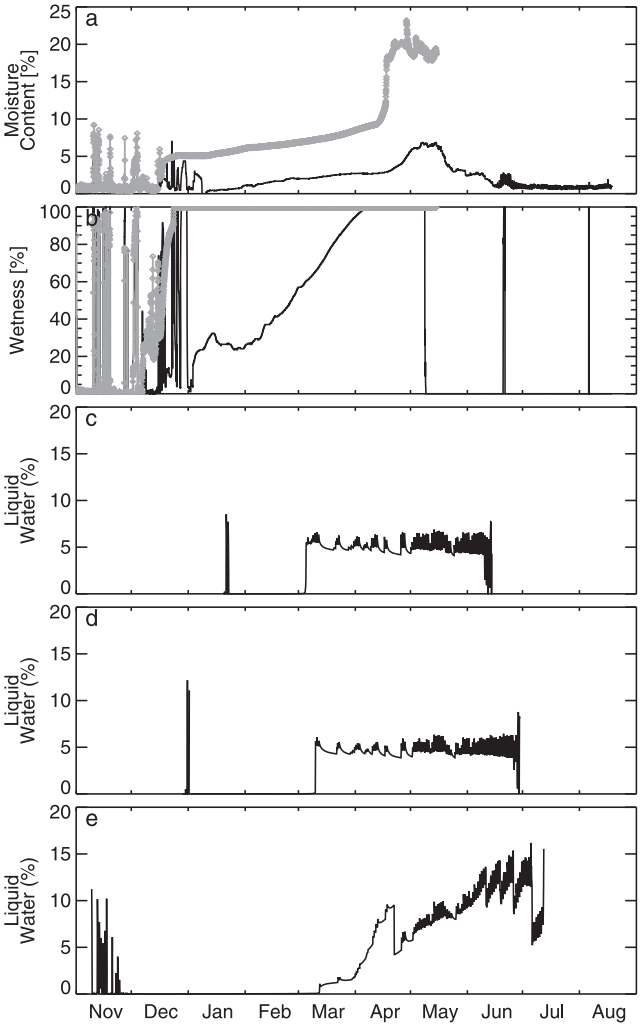

FIGURE 7. (a) Moisture content (% liquid water content in surrounding volume) from an ECHO probe and (b) wetness (% of full scale) of the snowpack from a leaf wetness sensor at two locations: the lower sensors are represented by the gray diamonds and the upper sensors are represented by the solid black lines (see text for sensor heights; data from both lower sensors are lost due to loss of power in the last third of the season). Liquid water fraction at three representative heights [(c) 2 m, (d) 1 m, (e) at the ground] within a best fit SNTHERM simulation snowpack. All measurements and modeled data are reported hourly.

These models provide insight into the energy balance of the snowpack throughout the season. Observations indicated that the highest temperature sensor was uncovered on 14 June 2008, and that final ablation of the snowpack (as indicated by diurnal changes seen in the lowest temperature sensor readings, about 0.02 m above the ground) occurred on 6 July 2008. As determined by the temperature sensors, the ablation from about 2 m (our highest temperature sensor) to the ground took place over 23 days, and no precipitation was recorded at our site or at any of the nearby sites during this time span. From this, we estimated a linear snow loss rate of about 8.6 cm/day. In order to force the SNTHERM model to reproduce the observed timing of the decrease in snowpack depth and the ablation rate, we varied the amount of precipitation during the snow season, the density of the falling snow, and the albedo of the snowpack. These variations are described in more detail below.

Precipitation data used to initialize the SNTHERM simulations were recorded at the Mineral weather station (Table 3, chosen

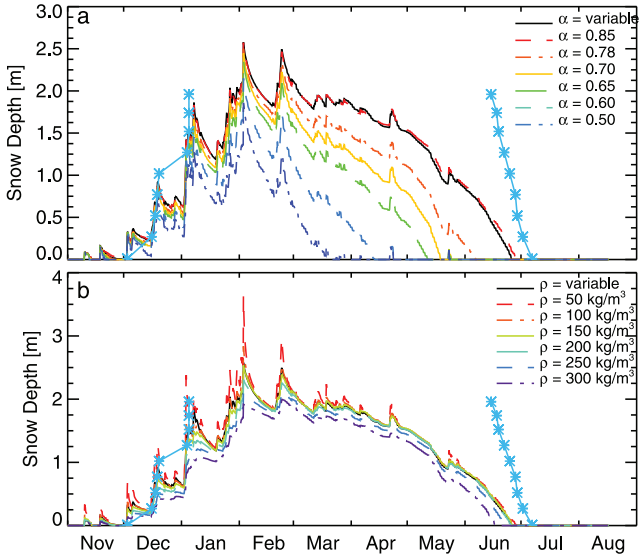

FIGURE 8. Comparison of SNTHERM simulated snow depth results for cases of (a) constant albedo and (b) constant snowfall density. Blue asterisks show the observed snow depths inferred from the TidbiT sensor data, as described in the text.

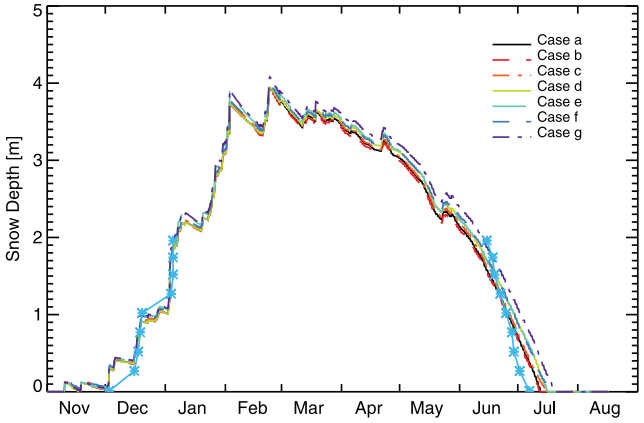

FIGURE 9. Comparison of SNTHERM simulated snow depths produced by varying multiple parameters. Each simulation's parameter values are listed in Table 5. Blue asterisks show the observed snow depths.

because the Lake Helen data was not available during this season). Mineral lies at a lower elevation and has different topographic surroundings, and so may have experienced different precipitation levels than those received at the fieldsite. Because initial simulations created snowpacks that were too shallow, we scaled the amount of precipitation recorded at the Mineral weather station by a constant amount throughout the season. The best fit models all utilize 1.9 times the amount of precipitation as Mineral, as this was found to produce the most accurate depths and timing of snowpack occurrence. Precipitation gradients with altitude have been calculated for the Sierra Nevada range (Meiman, 1970), although these gradients are not applicable to our region of study since local topography is likely to have greater influence in these two measurement areas. It is likely that individual precipitation events should be scaled separately, as meteorological conditions for each precipitation event determine the snowfall parameters and amount, but for our purposes, a uniform scaling was informative to provide approximations for total snowfall amounts.

ALBEDO

Albedo determines the amount of solar radiation transmitted into the snowpack, and is a key parameter in the SNTHERM simulations. Newly fallen snow typically has a high albedo, as high as 0.9 in pristine snow, because the snow grains are small and well-spaced. Albedo is lowered due to snowpack metamorphism, which decreases the pore space between snow grains and increases the grain size. The presence of larger snow grains lowers the albedo because the distance and travel time of light transmission is greater across a larger snow grain, which also acts to increase forward scattering within the snowpack so that light penetrates deeper (Curl et al., 1972; Wiscombe and Warren, 1980). Meltwater significantly lowers the albedo of snow, and the presence of contaminants with lower intrinsic albedo, such as dust and soot, may decrease the albedo to below 0.3, increasing absorption of solar radiation and providing more energy for melt.

In our numerical simulations, we either allowed the albedo to vary through time, as it naturally would due to the metamorphosis of the snowpack, or alternately defined it to remain at constant values. These albedo values couple the *measured* incident solar radiation to the *modeled* reflected solar radiation. High albedo, representing continued pristine snow, extends the lifetime of the snowpack, lowering the melting rate. Low albedo greatly reduces the duration of snow cover, as the melting rate is significantly higher due to the increased energy transmission into the snowpack (see Fig. 8, part a). If the albedo was allowed to vary with changes in modeled snowpack condition, SNTHERM predicted that the albedo only changed slightly throughout the whole season, with values falling between 0.7 and 0.8; however, we expect values at least as low as 0.5–0.6. This underestimate likely resulted from the model assumption of uncontaminated snow (as compared to the measured albedo that would include the effects of changes due to contaminants).

In a low-albedo snowpack model (α = 0.40; Fig. 8, part a), the simulated snowpack depth fell below 2 m on 3 February 2008, and the snowpack was completely ablated by 19 May 2008. The high-albedo snowpack, α = 0.85, was less than 2 m deep on 28 April 2008 and was completely ablated by 20 July 2008. Thus, we estimated the melt rate of low- and high-albedo snowpacks to be 4.6 cm/day and 2.4 cm/day, respectively, as compared with the observed snow ablation rate of 8.6 cm/day. Comparatively, the variable albedo base case fell below 2 m on 15 March 2008 and was completely ablated by 26 June 2008, giving an estimated melt rate of 1.9 cm/day.

DENSITY

There are three options for determining the density of newly fallen snow in SNTHERM: a model can be initialized with a constant density for falling snow; densities can be prescribed for each precipitation event; or the density can be modeled as a linear function of air temperature. Since we did not measure the density of the falling precipitation at the fieldsite, we ran simulations allowing the density to be modeled as a linear function of air temperature independently for each precipitation event, as well as simulations in which we set a constant experimental density (ranging from 30 to 300 kg/m^3) for the snowfall. We found that there were large differences in the total snowpack depth between these cases, with the low-density (30 kg/m^3) snowpack reaching a maximum depth of 4 m and the high-density (300 kg/m^3) snowpack peaking at 2 m (see Fig. 8, part b). However, initial snow density was quickly modified by compaction and metamorphosis once the snow was incorporated into the snowpack, so that the deep deposits that accumulated during precipitation events

TABLE 5

Parameters for the best-fit models shown in Figure 9.

Graph line	Graph color	Snow density (kg/m^3)	Snow albedo	Temperature change (°C)*	Day snow falls to 1.96 m	Day snow falls to 0.01 m	Ablation rate (cm/day)	Max Depth (m)
a	Black	325	0.62	−1.7	8 June	13 July	5.44	3.936
b	Red	325	0.62	−1.5	7 June	13 July	5.30	3.918
c	Orange	325	0.61	0	9 June	17 July	5.03	3.960
d	Yellow	325	0.67	−1.0	10 June	17 July	5.16	3.942
e	Green	299	0.67	−0.5	10 June	17 July	5.16	4.042
f	Blue	325	0.62	0	11 June	19 July	5.03	3.982
g	Purple	299	0.67	−1.0	14 June	20 July	5.30	4.078

* Temperature change from standard air temperatures taken from the camera box (as described in the text).

were quickly reduced to moderate snowpack depths between events. The high-density snowpack showed much less variation after individual events, as these precipitation densities were similar to that of the compacted, evolved snow. Because of the snow metamorphosis, the overall snow depth profile during the second half of the season was relatively similar between cases, with the final ablation of each simulated snowpack occurring within a range of 12 days. Thus, as seen in Figure 8, part b, the density of fresh snow had a significant effect on the overall depth of the snowpack during the season, but only a minor influence on the final date of melt. There was very little difference between the simulated snowpack ablation rates for these cases, with all of the simulations ablating at rates of about 5 cm/day, comparable to the rate of the snowpack with variable density.

MULTIPLE PARAMETER VARIATION

Modifying a single parameter within the SNTHERM simulations gives insight into the way that parameter manifests itself in the observable metamorphosis of a snowpack. However, snowpack growth, ablation, and timing are obviously affected by many physical parameters and it is necessary to simultaneously vary multiple parameters in the simulations in order to more accurately reproduce the LVNP observations. Unfortunately, due to the nature of the measurements available, many observable physical parameters remained unconstrained. Neither albedo nor density was measured, but both of these variables convey important information about the physical state of the snowpack. As described above, the albedo can vary naturally between 0.3 (low, absorbing) and 0.9 (high, reflective). The density can vary naturally between about 100 kg/m^3 (low; newly fallen snow) to 600 kg/m^3 (high; densely packed, mature snow). Factors such as the relative humidity, which were taken from other sites due to lack of data directly at Site A (see Table 3), were varied over a reasonable parameter range to determine their effect on the observed model variations, and were shown to have less of an effect on the snowpack metamorphosis than parameters such as albedo and density.

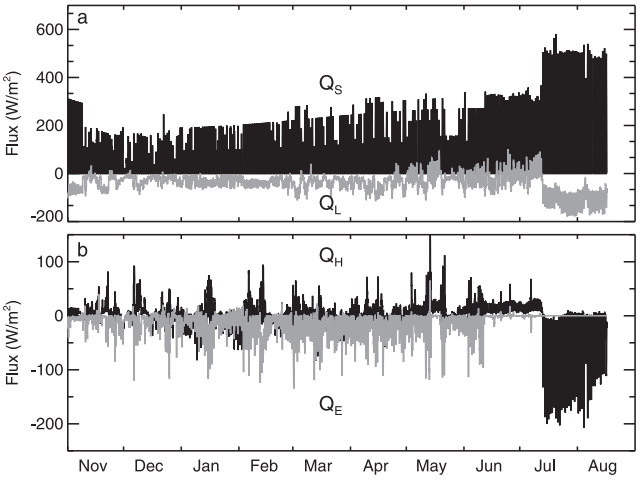

FIGURE 10. Hourly values for the main energy terms from a SNTHERM simulation (black line in Fig. 9). (a) Radiative flux terms, total solar radiation (Q_S, black line) and longwave radiation (Q_L, gray line). Longwave radiation becomes positive later in the season, primarily due to high air temperatures. (b) Turbulent flux terms, latent heat flux (Q_E, gray line) and sensible heat flux (Q_H, black line).

Because of the uncertainties in both the model and the data, we performed sensitivity studies to narrow down the parameter space of the variables that most strongly influenced the snowpack behavior. The most descriptive measured characteristic of the snowpack is temperature, which is also indicative of the timing of depth changes in the snowpack. Thus, within the simulated parameter space we attempted to reproduce the observed changes in temperature and snowpack growth and ablation timing with the SNTHERM models. Precipitation rates were scaled, as described above, for all of the following simulations. Initial snowfall density, snow albedo, and air temperature were adjusted in multiple configurations until a reasonable fit of the data was found. Variations from the nominal observed air temperatures were found to slightly shift the simulated depth profile in the latter half of the field season, so temperature can be used as a free parameter (within a few degrees) to slightly refine the timing. It is important to note that neither the density of falling snow nor the snowpack albedo are expected to be constant throughout the lifetime of a snowpack; however, setting these as constants allowed us to more clearly analyze their individual effects on the snowpack.

Figure 9 shows seven of the best-fit models whose parameters are listed in Table 5. As previously shown by the albedo and density data, wide variations in snowpack parameters can affect depth and timing of the snowpack. The best fits were determined by how well the ablation timing and slope matched the observations. By changing several parameters simultaneously, we saw that a variety of combinations could produce similar results. For instance, the green (e) and blue (f) lines were remarkably consistent throughout most of the simulation, yet were driven with quite different values for their key parameters. The simulation represented by the green line (e) had a snowfall density of 299 kg/m^3, α = 0.67, and the air temperature was shifted down from observations by 1.0 °C, while the simulation represented by the blue line (f) had a snowfall density of 325 kg/m^3, α = 0.62, and utilized the nominal air temperature. In all of the simulations

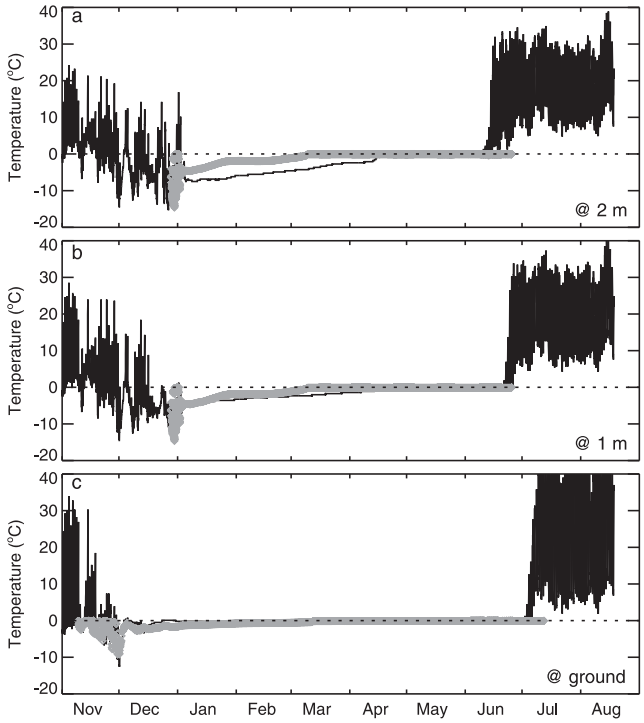

FIGURE 11. Comparison of hourly temperature profiles from the TidbiT observations (solid black line) with those predicted by a best-fit SNTHERM simulation (gray diamonds) at the given heights.

shown, the snowpack ablation from 2 m to the ground took 36–39 days (average rates of 5.0–5.4 cm/day).

In another case, the black line (a) in Figure 9 was obtained by implementing a snowfall density of 325 kg/m^3 and $\alpha = 0.62$, and subtracting 1.7 °C from the air temperature. This simulated snowpack fell to a depth of 2 m seven days before the observed drop to that height, and was completely ablated seven days after observations indicated that no snow remained on the ground around the sensors. This simulation had the shortest time span of the final 2 m of the snowpack, with an average ablation rate of about 5.4 cm/day (over 36 days). While this was still significantly lower than the observed rate (8.5 cm/day), it was the fastest ablation found in all of the simulations.

Although the details may vary, the general behavior of the snowpack was similar for each of the seven best-fit cases, and for the wider parameter space variations seen in Figure 8. From these simulations, we noted that the date and rate of the loss of snow were the most sensitive observables. By using these conditions, we constrained the values of such key parameters as albedo and density.

Discussion

ENERGY FLUXES

Snowpack metamorphosis is strongly dependent on the interior state of the snowpack as well as the driving external energy terms. Solar (shortwave) radiation is typically the dominant surface energy balance term (Cline, 1997a, 1997b; Dingman, 1994) driving heat transfer into a snowpack, as our models have also shown to be the case at LVNP. While there is some variety in the combinations of parameters that best reproduced the observed snowpack ablation results, these best-fit models all produced similar snowpack energy-balance results. It is

FIGURE 12. Early summer snow algae present at the fieldsite in Lassen Volcanic National Park (credit: Brian Duval, 2005).

constructive to look at the relative importance of the important energy-balance terms, as in Figure 10. For the model discussed above (black line (a) in Fig. 9), 92.8% of the total energy gain was input from solar radiation (Q_S), compared with the 7.2% from sensible heating (Q_H). Similarly, loss of longwave radiation (Q_L) from the snowpack contributed to 70.4% of the total energy lost from the system, while 29.6% was lost due to latent heating (Q_E). In Figure 10, it is readily apparent that radiative heating contributes the most energy to the snowpack throughout the season. In some of the parameter studies, changes in relative humidity were found to affect the contribution of latent energy to the snowpack surface energy balance, in which latent heat varied between about 17 and 30%. However, this was insignificant in affecting the overall energy balance, which remained dominated by the solar radiation term.

Although the predicted value for sensible heating may seem low, it is important to remember that the fieldsite is set in a valley which reduces the impact of the strong winds sometimes observed in the area. However, because the wind speed and temperature measurements are not directly from our fieldsite, it is possible that these energy-balance terms are weighted incorrectly. Other studies in the Sierra Nevada region observed that solar radiation accounts for 66–90% of energy available for melt during the snowmelt season, when latent and sensible heating terms may be strong but approximately cancel out (Marks and Dozier, 1992). At the "lake site" in Marks and Dozier (1992), the sensible heat contribution was greater than the radiant heat for the winter months (November–February), when the high albedo of the fresh, cold snow reduced the contribution from solar radiation; however, during the snowmelt season (March–July), radiant energy dominated. Similarly, Cline (1997a, 1997b) observed that the radiative fluxes contributed to 75% of the total energy available for snowmelt.

Using the basic equation for heat conduction, $Q_{cond} = -k_{th*}dT/dz$, we calculated the diffusive heat flow through the bottom meter of the snowpack after all of the sensors had been buried. Although the thermal conductivity of snow can vary over several orders of magnitude (Sturm et al., 1997), we chose a value on the high end, $k_{th} \approx 1$ W/m-K, to evaluate the case of efficient heat transfer through the snow. This yielded a heat flux of approximately 3.5 W/m^2 up through the bottom meter of the snow. The global average geothermal heat flux is about 0.075 W/m^2 (Pollack et al., 1993), but fluxes up to 94 W/m^2 have been

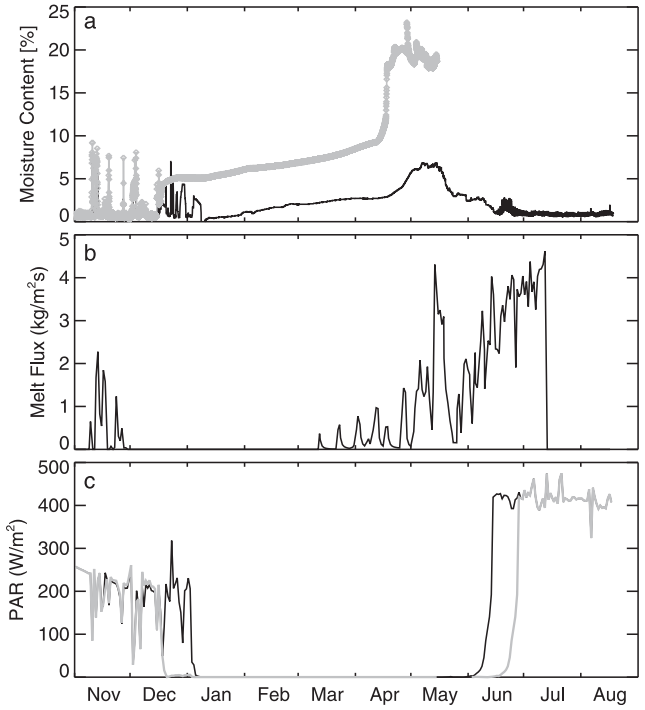

FIGURE 13. (a) Measured hourly ECHO moisture probe data for the tall post (dark gray lines) and short post (light gray lines) sensors. (b) Modeled daily maximum flux of meltwater at the snow-soil boundary. (c) Daily maximum measured incident solar radiation from the 1 m (gray lines) and 2 m (black line) sensors. The data from 2 m was collected over the entire season; however, the data collection at 1 m stopped in mid-May. Here, the gray line representing the 1 m solar radiation in June–September is shifted from that of the 2 m sensor based on modeled depth estimates.

observed in active geothermal areas in Yellowstone National Park (Watson et al., 2008). The calculated flux through the snow is a lower limit to the geothermal heat that is conducted up through the soil, but nevertheless indicates that geothermal heating was likely negligible compared to the hundreds of W/m^2 input into the snowpack from other energy sources for most of the season. However, the inclusion of this term, in addition to a darker albedo, might account for the more rapid disappearance of the snowpack at the end of the season, as a continual heat flow into the base of the snowpack will create melt once the lower snow layers are at 0 °C (Male and Gray, 1981).

OBSERVED AND MODELED SNOWPACK TEMPERATURE AND MOISTURE

As a final constraint on the validity of these models, we compared the simulated temperature and moisture content profiles with those measured in the snowpack throughout the observation season. Figure 11 shows the observed temperature profiles at three heights (1.96 m, 1.02 m, and 0.01 m) and the corresponding temperature profiles from a SNTHERM model. The onset of snow coverage of the sensors matched quite well with the observations, although as previously stated, the snow remained on the ground slightly longer in the simulation than was observed (this is apparent in the overshoot of the temperature data for the lowest sensor). In all three cases, the simulated snowpack became isothermal at 0 °C before the observations, but the exact dates of burial were slightly offset as well, and the trends of the temperatures were similar.

Figure 7 (parts c–e) shows the simulated liquid water fraction (LWF) in the snow at three layers, representing higher, middle, and lower regions of the modeled snowpack, respectively. Liquid water was present about 10 days earlier in the higher levels than at the bottom of the snowpack, but there was an overall increase in LWF toward the base of the snowpack. While we cannot quantitatively compare the LWF predicted by the model with our sensor measurements, we looked at the relationships between these three sets of data. ECHO moisture sensor observations from the fieldsite indicated a sharp increase in the moisture content at the lower sensor on 14 April 2008, and a similar increase was seen in the low-level moisture fraction of the simulated snowpack. In both the observations and the simulation, there was a sharp peak on 18 April 2008, along with comparable changes in relative moisture fraction. Additionally, the lower moisture sensor recorded higher moisture content earlier than the upper moisture sensor, but the models indicated that the opposite result should be observed. Models showed a peak in LWF when the snow was initially deposited, but then the higher layers increased in moisture content and showed only minor fluctuations throughout the rest of the life of the snowpack at that height, which was inconsistent with the slow rises observed by the moisture and wetness sensors. The modeled lowest layers showed more variation in LWF and a sharper rise, as was observed.

After rising throughout the winter, and then remaining steady throughout April, the higher wetness sensor data dropped to zero in May. This was due to a change in snowpack characteristics around the sensor. Although it is surprising that the data were recording zero wetness coverage, these readings may have indicated that the snowpack was ripe and water had begun to percolate down through the snowpack. Moisture sensor data may provide some support to this hypothesis, as the measured moisture content of the higher sensor had also leveled out and began to decrease a few days after this event. It is not clear from the data when the wetness sensor broke off of the tall post. After the precipitous drop in wetness coverage, spikes in the wetness data were observed on 19–20 June 2008 and 9–10 August 2008. These dates corresponded to the dates of precipitation events, and according to the TidbiT data there was likely about 10 cm of snow cover remaining above this sensor during the first event, so that the sensor was likely measuring the precipitation/melt percolating down through the top layers of the snowpack. The final spike may have been when the sensor broke off, or it may have simply measured precipitation as it occurred.

One complication of having the instrumentation along a single post is that the support structure itself may have formed a preferential pathway along which melt could flow. If the pores in the snow surrounding the post became saturated, a vertical channel could have formed which would then allow water to flow through the pores with increased efficiency (Male and Gray, 1981). Because the TidbiTs on the two different posts at similar heights were uncovered at about the same time, we do not believe there was a well forming around the posts, as is often observed around trees, which would affect all of the sensor readings. However, if a meltwater pathway formed along the metal posts, this might help explain the noted differences in liquid water content between the observations and the models. Additionally, the existence of a preferential pathway might explain the rapid loss of water around the wetness sensor on 9 May 2008.

POSSIBLE IMPLICATIONS FOR SNOW ALGAE

Also of interest is the relationship between the seasonal evolution of the snowpack and the presence of snow algae and timing of their movements. Although we do not have direct

indicators of the snow algae movement and timing for the 2007–2008 season, snow algae were possibly visible on camera images toward the end of the season, and have been observed at this site in the past (Steve Zachary, personal communication, and Fig. 12). The dominant factors controlling snow algae movement up through the snow are the availability of light and liquid water (Hoham, 1975). In Figure 13, measured incident solar radiation is compared to the liquid water content of the snowpack measured by the ECHO probes. The amount of liquid water in the snow was increasing throughout the spring, reaching at least 15% in early May; research indicates that snow algae are usually found in snow with 40–70% snow water equivalent (at least few percent to 10% liquid water) (Hoham and Ling, 2000).

Results from previous studies that focused on thinner snowpacks indicate that snow algae germination occurs in snowpacks of 30–40 cm thickness (Hoham, 1975; Hoham et al., 1983). However, these studies are not able to distinguish the parameter that controls the onset of germination. The onset may be initiated by the penetration of light through the snow, possibly related to the varying penetration depths of different wavelengths of light in snow, or by the timing of liquid water arrival in significant quantities at the bottom of the snowpack (where the algae lie dormant until germination). These variables are difficult to disentangle in the thin snowpacks studied because the increase of liquid water in the snowpack and light penetration at depth occur concurrently.

Light cannot penetrate to the ground for most of the snow-covered season in the thick snowpacks at Lassen. With our measurements and modeling, we can use the separation in timing between light and water arrival at depth in the snowpack to learn about the relationship between these two key variables and snow algae germination, and determine their relative importance. Because the snowpack at the Lassen site is so thick, the winter temperatures at the bottom of the snowpack are relatively warm (Fig. 11) and meltwater fraction throughout the snowpack increases long before light penetrates through the snowpack to reach the snow-soil interface (Fig. 13).

When the PAR sensor at 1 m was buried by approximately 0.25 m of snow it detected about 2% of the light collected by the 2 m PAR sensor. While some studies have predicted greater transmission (i.e., Schwerdtfeger and Weller, 1977), this factor is highly dependent on snow properties. Additionally, there may have been slightly higher transmission at blue wavelengths (where the scattering coefficient of ice is at a minimum) but the sensitivity of our PAR sensors drops off sharply toward the blue end of the visible spectrum (Onset Computer Corporation sensor manual #MAN-S-LIA). Applying this knowledge of the relationship between the 2 m and 1 m PAR sensors to the end of the observation season (where we did not have data from the 1 m sensor because the batteries died), we used the response of the 2 m PAR sensor and the approximately linear change in snow depth to predict the response of the PAR sensor at 1 m, shown in Figure 13. These observations and the SNTHERM models indicated that visible radiation reached 2 m above the ground in late May, approached 1 m above the ground in the middle of June, and that significant quantities of light did not reach the ground until late June.

Even allowing for the possibility of increased light penetration due to the high liquid water content (Curl et al., 1972; Wiscombe and Warren, 1980), the bottom of the snowpack at Lassen had significant quantities of liquid water some months before the light could reach this depth. From the SNTHERM models, we predict that melt began trickling down to the soil in mid-March (Fig. 13, part b), when there was melt occurring throughout the snowpack (see also Fig. 7). This indicates that if the snow algae were to germinate due to the presence of water, they would have then been able to migrate up through the meltwater in the snowpack to reach the necessary solar radiation levels of close to 0.1% of the full surface sunlight (Curl et al., 1972) that are found closer to the snow/air interface.

Conclusions

Instrumentation and observation methods utilized in this field study offer a simple and useful approach to *in situ* snow measurement, especially applicable at remote sites and in the case of thick, seasonal snowpacks. Analyses of thick snowpacks such as those at LVNP are important because they are an intermediate type of snow cover bridging the gap between a typical thin, seasonal snow cover and permanent snowfields and glaciers. Supplemental instrumentation is necessary in order to better constrain snowpack conditions and produce more useful data for driving snow models. This may include sensors to measure relative downwelling and upwelling solar radiation, terrestrial radiation, humidity, precipitation, and wind speed, which are all needed to drive the meteorological parameters used by SNTHERM. Additionally, comparison with snow pillow measurements would be useful for validation of variables such as snowpack water content and density.

Combining measurements taken at LVNP with numerical modeling has allowed us to more fully characterize the metamorphosis of the snowpack, and coordinate knowledge of snow algae growth with respect to the measured and predicted levels of water and light within the snowpack. These combined data sets are also useful for looking at long-term variability in snow cover and in snow cover duration. It is important to maintain observations of this kind at LVNP because snowpacks such as these likely run a significant risk of being affected by climate change (Déry and Brown, 2007; Brown and Mote, 2008), and greater understanding of the physical parameters and processes driving snowpack metamorphism may lead to better forecasting of runoff (a major water source for many areas), and also provide a better understanding of the feedback between snow cover and the global radiation budget.

Acknowledgments

This work was funded through the NASA Planetary Geology and Geophysics Program and a NASA Graduate Student Research Program Fellowship. We gratefully acknowledge the machine shop at NASA Ames Research Center for building the equipment stands, Lassen Volcanic National Park for access and permits for the site, Steve Zachary for invaluable help and guidance at the park, and the many field hands who have assisted in data collection over several field seasons. Additionally, we would like to thank the anonymous reviewers for their detailed comments and suggestions, which greatly improved the manuscript.

References Cited

Arya, S. P., 2001: *Introduction to Micrometeorology.* Second edition. San Diego: Academic Press.

Baker, K., 2001: Evaluation of PAR estimation methods. Rosemont, Illinois: Lake Michigan Air Directors Consortium, Technical Report.

Barnett, T. P., Pierce, D. W., Hidalgo, H. G., Bonfils, C., Santer, B. D., Das, T., Bala, G., Wood, A. W., Nozawa, T., Mirin, A. A., Caya, D. R., and Dettinger, M. D., 2008: Human-induced changes in the hydrology of the western United States. *Science*, 319: 1080–1083.

Brown, R., and Mote, P., 2008: The response of northern hemisphere snow cover to a changing climate. *Journal of Climate*, 22: 2124–2145.

California Department of Water Resources California Data Exchange Center (CDEC), 2010, Available at http://cdec.water.ca.gov/, accessed 23 December 2010.

Cline, D., 1997a: Snow surface energy exchanges and snowmelt at a continental, midlatitude alpine site. *Water Resources Research*, 33: 689–701.

Cline, D., 1997b: Effect of seasonality of snow accumulation and melt on snow surface energy exchanges at a continental alpine site. *Journal of Applied Meteorology*, 36: 32–51.

Cline, D., Yueh, S., Chapman, B., Stankov, B., Gasiewski, A., Masters, D., Elder, K., Kelly, R., Painter, T. H., Miller, S., Katzberg, S., and Mahrt, L., 2009: NASA Cold Land Processes Experiment (CLPX 2002/03): Airborne Remote Sensing. *Journal of Hydrometeorology*, 10: 338–346.

Curl, H. Jr, Hardy, J. T., and Ellermeier, R., 1972: Spectral absorption of solar radiation in alpine snowfields. *Ecology*, 53: 1189–1194.

Déry, S., and Brown, R., 2007: Recent northern hemisphere snow cover extent trends and implications for the snow-albedo feedback. *Geophysical Research Letters*, 34: L22504, doi:10.1029/2007GL031474.

Dingman, S. L., 1994: *Physical Hydrology*. New York: Macmillan Publishing Company.

Edwards, H. G. M., de Oliveira, L. F. C., Cockell, C. S., Ellis-Evans, J. C., and Wynn-Williams, D. D., 2004: Raman spectroscopy of senescing snow algae: pigmentation changes in an Antarctic cold desert extremophile. *International Journal of Astrobiology*, 3: 125–129.

Elder, K., Cline, D., Goodbody, A., Houser, P., Liston, G., Mahrt, L., and Rutter, N., 2009a: NASA Cold Land Processes Experiment (CLPX 2002/03): ground-based and near-surface meteorological observations. *Journal of Hydrometeorology*, 10: 330–337.

Elder, K., Cline, D., Liston, G., and Armstrong, R., 2009b: NASA Cold Land Processes Experiment (CLPX 2002/03): field measurements of snowpack properties and soil moisture. *Journal of Hydrometeorology*, 10: 320–329.

Groisman, P., Karl, T., and Knight, R., 1994: Observed impact of snow cover on the heat balance and the rise of continental spring temperatures. *Science*, 263: 198–200.

Hardy, J. T., and Curl, H. Jr, 1972: The candy-colored, snow-flaked alpine biome. *Natural History*, 81: 74–78.

Hayashi, M., Hirota, T., Iwata, Y., and Takayabu, I., 2005: Snowmelt energy balance and its relation to foehn events in Tokachi, Japan. *Journal of the Meteorological Society. Japan*, 83: 783–798.

Hoham, R., and Ling, H., 2000: Snow algae: the effects of chemical and physical factors on their life cycles and populations. *In* Seckbach, J. (ed.), *Journey to Diverse Microbial Worlds: Adaptation to Exotic Environments*. Boston: Kluwer Academic Publishers, 131–145.

Hoham, R., Mullet, J., and Roemer, S., 1983: The life history and ecology of the snow alga *Chloromonas polyptera* comb. nov. (Chlorophyta, Volvocales). *Canadian Journal of Botany*, 61: 2416–2429.

Hoham, R. W., 1975: The life history and ecology of the snow alga *Chloromonas pichinchae* (Chlorophyta, Volvocales). *Phycologia*, 14: 213–226.

Hoham, R. W., 1980: Unicellular chlorophytes—Snow algae. *In* Cox, E. R. (ed.), *Phytoflagellates*. New York: Elsevier/North Holland, 61–84.

Jin, J., Gao, H., Yang, Z.-L., Bales, R., Sorooshian, S., Dickinson, R., Sun, S., and Wu, G., 1999: Comparative analyses of physically based snowmelt models for climate simulations. *Journal of Climate*, 12: 2643–2657.

Jordan, R., 1991: *A one-dimensional temperature model for a snow cover*. Hanover, New Hampshire: U.S. Army Cold Regions Research and Engineering Laboratory (CRREL), Special Report 91–16.

Lassen Volcanic National Park, 2010: U.S. Department of the Interior, National Park Service. Available at http://www.nps.gov/lavo/index. Last accessed 23 April 2010.

Lundquist, J. D., and Lott, F., 2008: Using inexpensive temperature sensors to monitor the duration and heterogeneity of snow-covered areas. *Water Resources Research*, 44: W00D16, doi:10.1029/2008WR007035.

Male, D. H., and Gray, D. M., 1981: Snowcover ablation and runoff. *In* Gray, D. M., and Male, D. H. (eds.), *Handbook of Snow*. New York: Pergamon Press, 360–436.

Marks, D., and Dozier, J., 1992: Climate and energy exchange at the snow surface in the alpine region of the Sierra Nevada 2. Snow cover energy balance. *Water Resources Research*, 28: 3043–3054.

McKay, C. P., Friedmann, E. I., Gómez-Silva, B., Cáceres-Villanueva, L., Andersen, D. T., and Landheim, R., 2003: Temperature and moisture conditions for life in the extreme arid region of the Atacama Desert: four years of observations including the El Niño of 1997–1998. *Astrobiology*, 3: 393–406.

Meiman, J. R., 1970: Snow accumulation related to elevation, aspect, and forest canopy. *In: Snow Hydrology: Proceedings of the Workshop Seminar, University of New Brunswick*, 35–47.

Müller, T., Leya, T., and Fuhr, G., 2001: Persistent snow algal fields in Spitsbergen: field observation and a hypothesis about the annual cell circulation. *Arctic, Antarctic, and Alpine Research*, 33: 42–51.

Painter, T. H., Duval, B., Thomas, W. H., Mendez, M., Heintzelman, S., and Dozier, J., 2001: Detection and quantification of snow algae with an airborne imaging spectrometer. *Applied and Environmental Microbiology*, 67: 5267–5272.

Pollack, H. N., Hurter, S. J., and Johnson, J. R., 1993: Heat flow from the Earth's interior: analysis of the global data set. *Reviews of Geophysics*, 31: 267–280.

PRISM Climate Group, 2006: Prism Climate Group State Maps. Oregon State University. Available at http://www.prism.oregonstate.edu/state_products/?id=CA (last accessed 15 December 2010).

Schwerdtfeger, P., and Weller, G. E., 1977: Radiative heat transfer processes in snow and ice. *In* Businger, J. A. (ed.), *Meteorological Studies at Plateau Station, Antarctica*. Washington, DC: American Geophysical Union, Antarctic Research Series, 25: 35–39.

Selker, J. S., Thevenaz, L., Huwald, H., Mallet, A., Luxemburg, W., de Giesen, N. v., Stejskal, M., Zeman, J., Westhoff, M., and Parlange, M. B., 2006: Distributed fiber-optic temperature sensing for hydrologic systems. *Water Resources Research*, 42: W12202, doi:10.1029/2006WR005326.

Stanhill, G., and Fuchs, M., 1977: The relative flux density of photosynthetically active radiation. *Journal of Applied Ecology*, 14: 317–322.

Sturm, M., Holmgren, J., Konig, M., and Morris, K., 1997: The thermal conductivity of seasonal snow. *Journal of Glaciology*, 43: 26–41.

Taras, B., Sturm, M., and Liston, G. E., 2002: Snow-ground interface temperatures in the Kuparuk River Basin, Arctic Alaska: measurements and model. *Journal of Hydrometeorology*, 3: 377–394.

Tyler, S. W., Burak, S. A., McNamara, J. P., Lamontagne, A., Selker, J. K., and Dozier, J., 2008: Spatially distributed temperatures at the base of two mountain snowpacks measured with fiber-optic sensors. *Journal of Glaciology*, 54: 673–679.

Watson, F. G. R., Lockwood, R. E., Newman, W. B., Anderson, T. N., and Garrott, R. A., 2008: Development and comparison of Landsat radiometric and snowpack model inversion techniques for estimating geothermal heat flux. *Remote Sensing of Environment*, 112: 471–481.

Wharton, R. A. Jr., and Vinyard, W. C., 1983: Distribution of snow and ice algae in western North America. *Madrofo*, 30: 201–209.

Wiscombe, W. J., and Warren, S. G., 1980: A model for the spectral albedo of snow. I: Pure snow. *Journal of the Atmospheric Sciences*, 37: 2712–2733.

Yoshimura, Y., Kohshima, S., and Ohtani, S., 1997: A community of snow algae on Himalayan glacier: change of algal biomass and community structure with altitude. *Arctic and Alpine Research*, 29: 126–137.

MS accepted July 2011